ngVLA Antenna Memo # 7

Axially Corrugated Feed Horns as Radiators for the 1.2 to 12.3 GHz Frequency Range on the ngVLA Reference Design Antenna

Sivasankaran Srikanth, Central Development Laboratory, Charlottesville, VA

June 16, 2020.

Abstract

The quad-ridged flared horn is the current choice of feed for Bands 1 and 2 on the ngVLA Design #6 antenna. This memo examines the performance of the antenna when fed by axially corrugated feed horns for these two bands. This horn has an aperture diameter comparable to that of the quad-ridged horn. It is simple in construction, easier to machine and would cost less. Performance results of two variations of the quad-ridged horn at Band 2 are shown. When the axially corrugated horn is directly substituted for Bands 1 and 2, efficiency drop-off at the high end of the bands is substantial compared to that of the quad-ridged horn. Using three axially corrugated horns to cover the frequency range of 1.2-12.3 GHz, the average efficiency is 85%. However, the third receiver results in increased construction, maintenance and operational costs.

1 Introduction

It is envisioned that the ngVLA project will have ten times the sensitivity of the JVLA and ALMA, and will cover the frequency range of 1.2 to 116 GHz. The main array will have baselines up to 1000 km that yield mas-resolution with extended baselines up to nearly 9000 km. The chosen antenna diameter of 18 m is a balance of several factors such as cost and operations constraints, imaging capabilities, survey speed, field of view, and the technological risk of the post-processing systems [1]. The current optics is a dual-offset Gregorian antenna with shaped reflectors [2]. This design provides comparatively larger real estate for housing all the receivers, compared to a symmetric antenna. In addition, the offset design provides high gain, low sidelobes and minimized standing waves. Because of the limited space and weight constraints on an 18-m antenna, the number of dewars and receiver bands had to be kept at a minimum. The specified frequency range is serviced with six receivers housed in two dewars [3]. Since the size of the feed horn is inversely proportional to the subreflector subtended angle, the reference design has a large opening angle (half-angle) of θ_s=55º. The frequency bands are shown in Table 1 [3].

2 Reference design six-band solution

Bands 1 and 2 have bandwidth ratios of 2.92:1 and 3.51:1, respectively. The plan is to use quad-ridged flared horns (QRFH) [4], [5], [6] for these two bands. The QRFH has orthogonal coaxial outputs and does not require an orthomode transducer (OMT) for extracting the two linearly polarized signals. As shown in Table 1, Bands 3-6 have bandwidth ratio of 1.68:1, where the bandwidth is limited by the available polarizer. Turnstile junction OMTs [7] or Boifot type OMTs [8], both developed at NRAO, have been successfully used in receivers on the GBT, VLA, VLBA, ALMA and various other telescopes to cover frequencies above 12 GHz. A double-ridged Boifot junction OMT design [9] meets the bandwidth specifications of the Band 6 receiver on the ngVLA. The axially corrugated feed horn (ACFH) [10], [11], [12] is the choice of feed for Bands 3-6. This horn has an aperture diameter of about 2λ at the low end of the band, while the diameter of QRFH varies between 1.5λ and 3.5λ.

3 Two-band solution for the 1.2 to 12.3 GHz range with QRFH

Bands 1 and 2 cover the 1.2 to 3.5 GHz and 3.5 to 12.3 GHz frequency ranges, respectively. At least two different groups were contracted to develop a design for wideband feed for Band 2, this being the one with a wider bandwidth of the two receivers. EMSS Antennas from South Africa, one of the groups, released their report on an all-metal QRFH solution in November 2019 [13]. The horn and ridge contours in their design have analytic profiles. Nine parameters defining the horn were varied for optimizing return loss (S_{11}) and system temperature over aperture efficiency (T_{sys}/η_a). Figure 1(a) shows the design of the horn which has an aperture diameter of 304 mm and an overall length of 302 mm. The diameter and length are 3.55λ and 3.52λ, respectively, at 3.5 GHz. Return loss is shown in Figure 1(b) and is better than -18 dB except at the band edges. CST Microwave Studio simulated patterns are shown at four frequencies in Figure 2. Copolar patterns are shown in three planes and crosspolar patterns in the 45º-plane. The illumination taper at 55º varies between -10 and -18 dB in the E-plane, while the variation in the H-plane is much larger (-15 to -40 dB). The worst crosspolarization is -15 dB below the peak of the copolarized beam. The first sidelobe of the ngVLA antenna pattern simulated in GRASP, varies between -13 dB and -19 dB and crosspolarization is better than -21 dB, as shown in Figure 3. Computed aperture efficiency is shown in Figure 4. It decreases monotonically from a value of 80% at 3.5 GHz to about 63% at 12.3 GHz. This is consistent with the narrowing of the feed pattern at higher frequencies.

The second contractor is CSIRO in Australia. Their final report was also submitted in October 2019 [14]. Results extracted from their report are summarized here. The feed horn is a dielectrically-loaded quad-ridged horn designed to achieve the specified 3.51:1 bandwidth. The report includes the necessary design elements required for cryogenic operation and shows results of thermal analysis carried out to show the viability of cooling the feed horn. The feed horn shown in Figure 5(a) has a central PTFE dielectric spear that concentrates the field at the higher frequencies towards the center of the horn. The concentric grooves on the outer section of the horn controls the beam shape at the lower frequencies. The diameter of the horn is 152mm which is 1.8λ at 3.5 GHz. The reflection coefficient shown in Figure 5(b) is the combined results of the horn and the OMT and is better than 17 dB. Patterns of the feed horn simulated in HFSS are shown in Figure 6 at four frequencies. The match between the E- and H-plane patterns is good, especially within the subreflector subtended angle. Crosspolarization in the 45º-plane is better than -21 dB. The antenna patterns in three planes are shown in Figure 7 and the beam symmetry is excellent. Crosspolarization shown in the 45º-plane is caused by the feed polarization. The first sidelobe is about -17 dB on the average and the worst crosspolarization is -24 dB (Figure 8). Aperture efficiency of the antenna is shown in Figure 9. Efficiency at 3.5 GHz is 86% and the average efficiency over the frequency band is 87%. As per the report, the structure seen in the efficiency plot is caused by scattering and reflections off of the corrugations at the high end of the frequency spectrum. This design with the central dielectric spear and the corrugations on the exterior is much more complex and likely costlier compared to the horn designed by EMSS Antennas. This design certainly results in superior performance over the large bandwidth of 3.5:1.

4 Two-band solution of the 1.2 to 12.3 GHz range with ACFH

Linear taper corrugated horns with narrow flare angles $\theta_f \leq 20^\circ$ and aperture diameters $\geq 8\lambda$ (at the low frequency end) have constant beamwidth over 2:1 bandwidth. These horns have illumination tapers between -12 dB and -15 dB, at angles close to θ_f. The beamwidth is a function of θ_f and is said to be functioning on flare-angle control mode. Wide flare angle horns with relatively small diameters used at

prime focus are said to operate on aperture-control mode. The radiation patterns of these horns have illumination taper of about -12 dB at the edge of the reflector and have much lower bandwidth (1.3:1).

The ACFH proposed for Bands 3 and higher has $\theta_f = 55^o$ and aperture diameter of 2λ (at the low frequency end) [15]. The pattern has illumination taper -15 to -16 dB at the edge of the subreflector. Figure 10 shows dimensions of an ACFH for the1.2 to 2.4 GHz range. The aperture (inside) diameter is 489 mm and the horn is 250 mm long. Figure 11 illustrates half-beamwidth at levels of -15 dB and -18 dB as a function of frequency in three planes. In the 1.2 to 2.15 GHz range, the -15 dB (Figure 11(a)) and -18 dB (Figure 11(c)) beamwidths vary from 55^o to 48^o (12.6%) and 62^o to 53^o (15.6%), respectively. Over this 1.8:1 band this horn works in the flare-angle control mode. In the following paragraphs, the performance of the above horn on the ngVLA antenna over wider bandwidths, for instance at Bands 1 and 2, are shown. For frequencies between 2.5 and 3.5 GHz, the beamwidth of the horn changes by a large amount as seen in Figures 11(b) and (d) as the horn is operating in the aperture-control mode.

Simulated return loss is better than -20 dB above 1.3 GHz (Figure 12(a)) and crosspolarization level is below -20 dB up to 2.6 GHz (Figure 12(b)). Above 2.6 GHz, crosspolarization is nearly -20 dB, with the exception of a small band (2.6 to 3.0 GHz). Copolar beam patterns are shown in Figure 13 in three planes. Crosspolarization is maximum in the D-plane (blue trace). The beam is circularly symmetric with constant beamwidth up to 2.1 GHz and the crosspolarization is below -30 dB. At higher frequencies, the beam becomes elliptical and the level of crosspolarization increases. Examining the phase center travel as a function of frequency, the average phase center distance is -120 mm from the aperture of the horn. Antenna patterns of the ngVLA are calculated for the above phase center location. Patterns are shown in three planes in Figure 14. The 0^o-plane (black and blue traces) is the symmetric plane of the antenna. At frequencies $\leq$2.1 GHz, the antenna induced crosspolarization (cyan trace) is about the same as that caused by the feed crosspolarization (purple trace). At higher frequencies, crosspolarization is dominated by the feed polarization. Aperture efficiency is shown in Figure 15. Efficiency is $\geq$82% from 1.2 to 2.8 GHz, and then decreases monotonically to about 48% at 3.5 GHz.

Since Band 2 has higher bandwidth (3.51:1) requirement, the scaling from the Band 1 feed shown in the previous section, is a balance between efficiency at the high end of the band (3.5 GHz) and return loss at the low end (1.2 GHz). The scaling factor used was 3.6/12.3. The feed, shown in Figure 16, has an aperture diameter of 143 mm (1.8λ at 3.5 GHz) and length of 75 mm. Return loss at 3.5 GHz is -8.0 dB and crosspolarization above 8.7 GHz varies between -15 dB and -20 dB as shown in Figure 17. Simulated patterns of the feed are shown in Figure 18. Patterns at 4.1 GHz (not shown) are identical to the patterns at 1.2 GHz shown in Figure 13(a). The pattern is circularly symmetric up to 7.18 GHz. Figure 19 shows antenna beam patterns. The horn was located with its aperture 35 mm in front of the secondary focus. Crosspolarization is dominated by the feed polarization at all the frequencies shown. Aperture efficiency is shown in Figure 20 and is very similar to the efficiency in Figure 15. The ACFH has superior performance compared to the EMSS QRFH from 3.5 to 10.0 GHz. At higher frequencies, the QRFH has about 13% higher efficiency. The ACFH has performance very similar to that of the CSIRO QRFH up to 9.0 GHz but degrades at higher frequencies. However, the ripple seen in the CSIRO horn is absent, which may be an advantage.

The phase center location used in the above two cases, favor frequencies at the upper end of the band. It should be noted that the ACFHs will require a broadband OMT to extract the two orthogonal polarizations. The OMT is an integral part of the two QRFHs designed by EMSS Antennas and CSIRO.

5 Three-band solution of the 1.2 to 12.3 GHz range with ACFH

If construction, operation and maintenance cost and space availability were not limiting factors, best performance could be achieved by using three bands to cover the 1.2 to 12.3 GHz frequency span. In Figure 15, aperture efficiency is consistently above 82% in the 1.2 to 2.7 GHz range and this band is designated “Band 1” in this solution. Using a similar bandwidth ratio, excellent efficiency could be achieved by dividing the rest of the range into two bands covering 2.7 to 5.8 GHz (Band 2a) and 5.8 to 12.3 GHz (Band 2b), respectively.

The ACFH for Band 2a is 217 mm in diameter and 130 mm long as shown in Figure 21. Return loss is better than -20 dB for frequencies above 2.8 GHz and crosspolarization is lower than -20 dB (Figure 22). The feed patterns show good circular symmetry up to 5.0 GHz, as seen in Figure 23. The phase center is located at 63 mm from the aperture and this position is used in the GRASP analysis. Antenna beam patterns are shown in Figure 24 and crosspolarization is better than -26.5 dB. Aperture efficiency varies between 81% and 87% (Figure 25).

Figures 26 to 30 cover feed horn dimensions, input return loss, maximum crosspolarization, simulated patterns of the feed, antenna beam patterns and efficiency for Band 2b. The phase center position used in the GRASP analysis is 29 mm behind the aperture of the horn. Aperture efficiency is higher than 83% in the entire frequency range. The three bands also require OMTs but with lower bandwidth requirement.

Figure 31 shows the two ACFHs covering the 1.2-3.5 GHz and 3.5-12.3 GHz ranges. Figure 32 shows the horns for the 1.2-2.7 GHz, 2.7-5.8 GHz and 5.8-12.3 GHz ranges. The drawings are to scale and hence give a perception of the relative sizes.

6 Conclusions

Performance results of the Band 2 QRFH designed by EMSS Antennas and CSIRO are presented in this memo. The CSIRO design uses a dielectric spear that results in better performance at the high end of the band and corrugations to reduce spillover at the low end. Efficiency on the antenna with this feed is higher than 80%. This memo shows the radiation characteristics of ACFHs directly substituted for the proposed QRFHs for Band 1 and 2. ACFH for Band 2 has better performance from 3.5 to 10.0 GHz compared to EMSS QRFH. Above 10.0 GHz, the QRFH has 13% higher efficiency on the average. The ACFH has very similar efficiency from 3.5 to 9.0 GHz as the CSIRO horn and is inferior at higher frequencies. The ripples present in the efficiency plot of the QRFH may have adverse effects in some observations.

This memo also presents results using three ACFHs to cover the 1.2 to 12.3 GHz range. This option results in aperture efficiency higher than 81% over the entire range. However, it requires an extra receiver, with increase in construction, operation and maintenance costs. Using ACFHs results in the need for OMTs that need to be developed.

The author acknowledges P. Ward, R. Selina, E. Murphy and W. Grammer for their valuable and constructive suggestions and edits.

References

[1] R. Selina, “System-level Cost Comparison of Offset and Symmetric Optics,” ngVLA Antenna Memo #1, May 24, 2019, VI.I.

[2] L. Baker, “Analysis of ngVLA Design #6 With Ideal and Actual Feed,” Document # 020.25.01.00.00_0001-REP ngVLA Optical Reference Design, January 2017.

[3] W. Grammer et al., “ngVLA Front End Reference Design Description,” Document # 020.30.03.01.00-0003-DSN.

[4] A. Akgiray, S. Weinreb, W. A. Imbriale and C. Beaudoin, “Circular Quadruple-Ridged Flared Horn Achieving Near-Constant Beamwidth Over Multiocatave Bandwidth: Design and Measurements,” IEEE Trans. Antennas Propag., Vol. 61, No. 3, pp. 1099-1108, Mar. 2013.

[5] J. Shi, S. Weinreb, W. Zhong and X. Yin, “Quadruple-Ridged Flared Horn Operating from 8 to 50 GHz,” Internal Memo, Dept. of Electrical Engineering, California Institute of Technology, Pasadena, CA, December 1, 2016.

[6] A. Dunning, M. Bowen, M. Bourne, D. Hayman and S. L. Smith, “An ultra-wideband dielectrically loaded quad-ridged feed horn for radio astronomy,” in Proc. IEEE-APS Conf. Antennas Propag. Wireless Communic. (APWC 2015), Turin, Italy, Sept. 2015, pp. 787-790.

[7] Sivasankaran Srikanth and Miles Solatka, “Wideband Orthomode Transducer for Millimeter Bands,” 2013 Asia-Pacific Radio Science Conference, Taipei, Taiwan, Sept. 3-7, 2013.

[8] E. Wollack, “A Full Waveguide Band Orthomode Junction,” Electronics Division Internal Report, National Radio Astronomy Observatory, Green Bank, WV, no. 303, May 1996.

[9] A. Gonzalez and S. Asayama, “Double-Ridged Waveguide Orthomode Transducer (OMT) for the 67-116 GHz Band,” Journal of Infrared, Millimeter, and Terahertz Waves 39, pp. 723-737, 14 June 2018.

[10] Z. Ying, A.A. Kishk and P.–S. Kildal, “Broadband compact horn feed for prime-focus reflectors,” ELECTRONICS LETTERS, 16 July 1995, Vol. 31, No. 14, pp. 1114-1115.

[11] R. Lehmensiek and D. I. L. de Villiers, “Wide Falre Angle Axially Corrugated Conical Horn Design for a Classical Offset Dual-Reflector Antenna,” 6th European Conference on Antennas and Propagation (EUCAP) 2012.

[12] L. Baker and B. Veidt, “DVA-1 Performance with An Octave Horn from CST and GRASP Simulations,” octave_horn_rpt.nb, 03/30/2014.

[13] R. Lehmensiek, “ngVLA: Band 2 Feed Study, Final Report,” EMSS Antennas Doc Number: EA-NGV-DR-04, 7 November 2019.

[14] A. Dunning, N. Carter and S. Smith, “Design of a Band 2 Feed Horn for the ngVLA. Study II: Dielectrically-loaded quad-ridged feed horn,” CSIRO 30/10/2019.

[15] L. Baker and B. Veidt, “DVA-1 Performance with an Octave Horn from CST & GRASP Simulations,” octave_horn_rpt.nb, 03/30/2014.

Table 1.

Band	1	2	3	4	5	6
Frequency (GHz)	1.2-3.5	3.5-12.3	12.3-20.5	20.5-34.0	30.5-50.5	70.0-116.0
Bandwidth ratio	2.92:1	3.51:1	1.67:1	1.66:1	1.66:1	1.66:1
Feed type	QRFH	QRFH	ACFH	ACFH	ACFH	ACFH

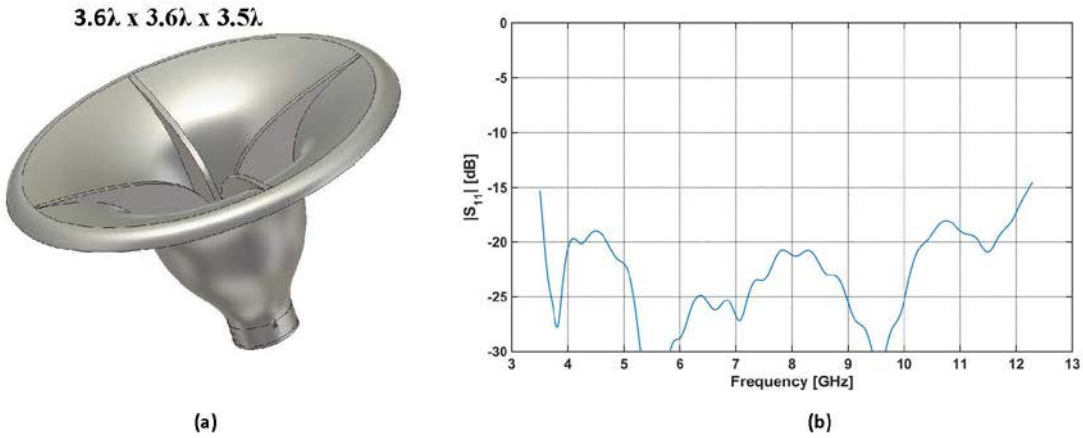

Figure 1. (a) EMSS Quad-ridged flared horn (QRFH), (b) Return loss.

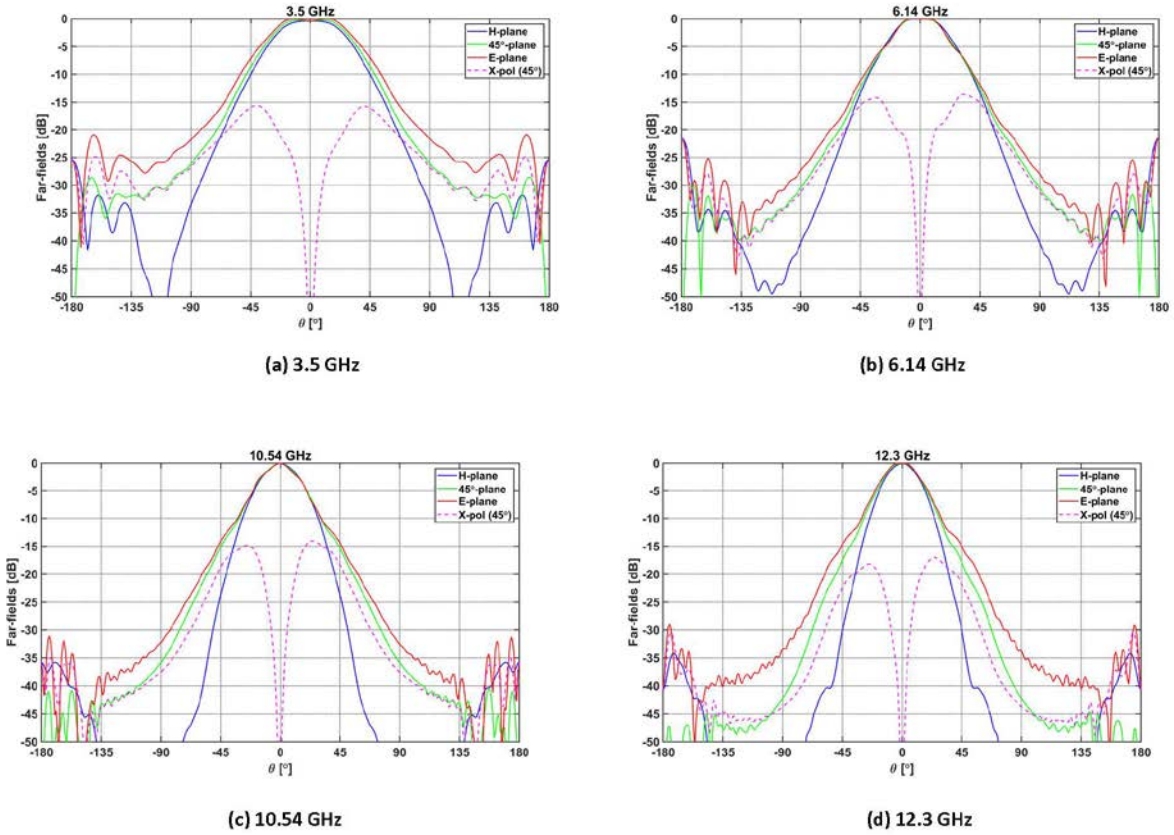

Figure 2. Simulated feed patterns of the EMSS QRFH.

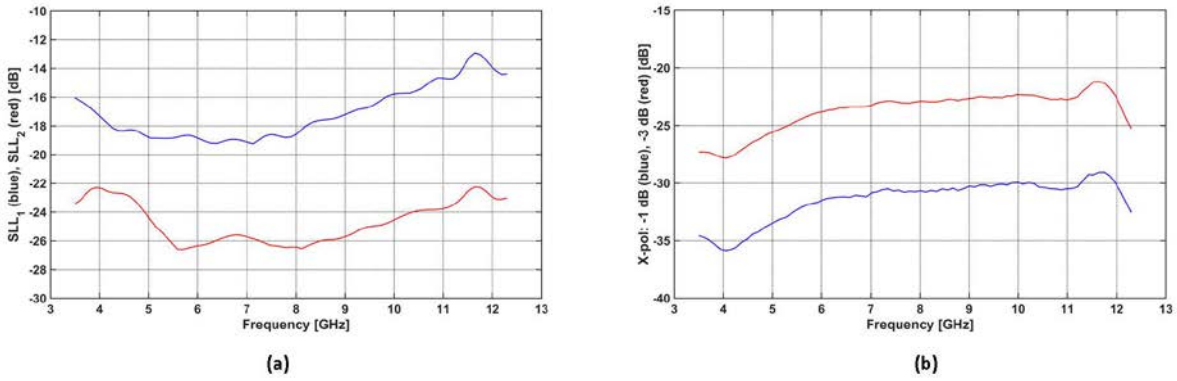

Figure 3. (a) 1st and 2nd sidelobe levels of the antenna pattern, (b) Crosspolarization within -1 dB and -3 dB off copolarization peak.

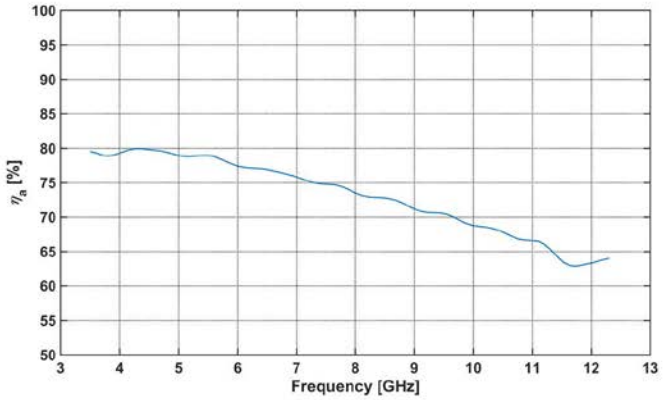

Figure 4. Aperture efficiency of the antenna with the EMSS QRFH.

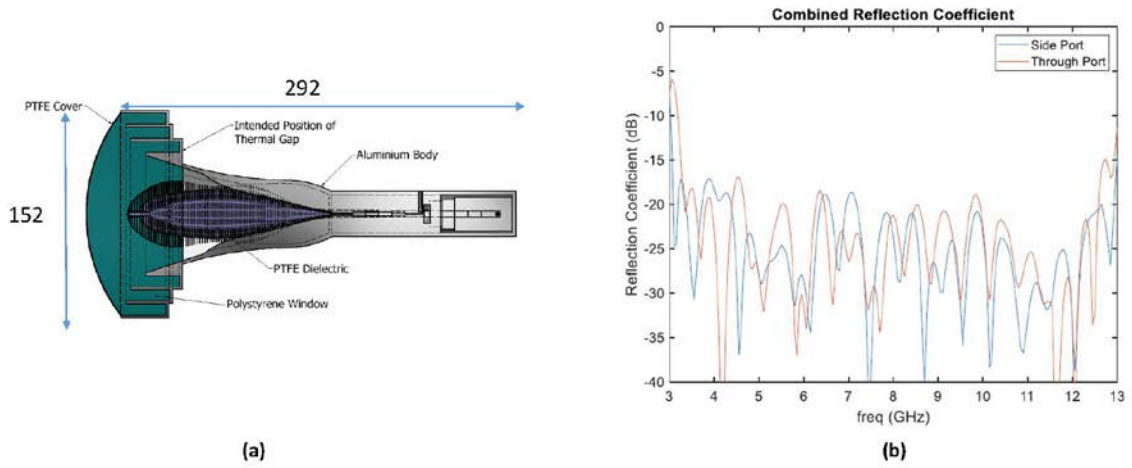

Figure 5. (a) CSIRO Quad-ridged flared horn with dielectric insert, (b) Input reflection coefficient.

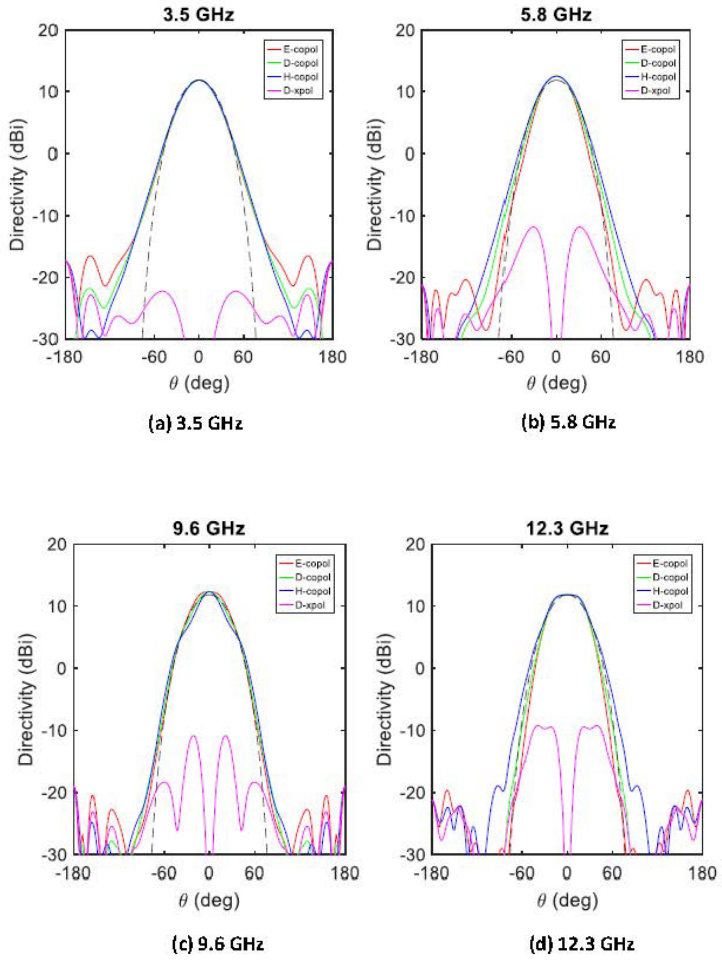

Figure 6. Simulated patterns of the CSIRO QRFH.

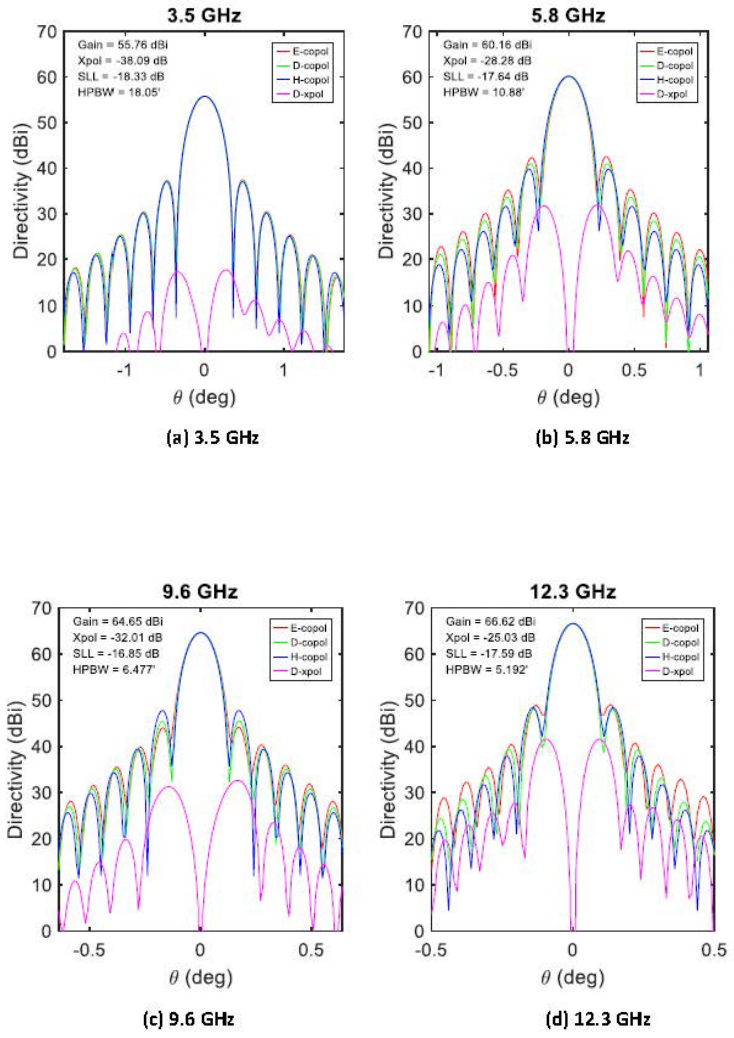

Figure 7. Simulated antenna patterns with the CSIRO QRFH.

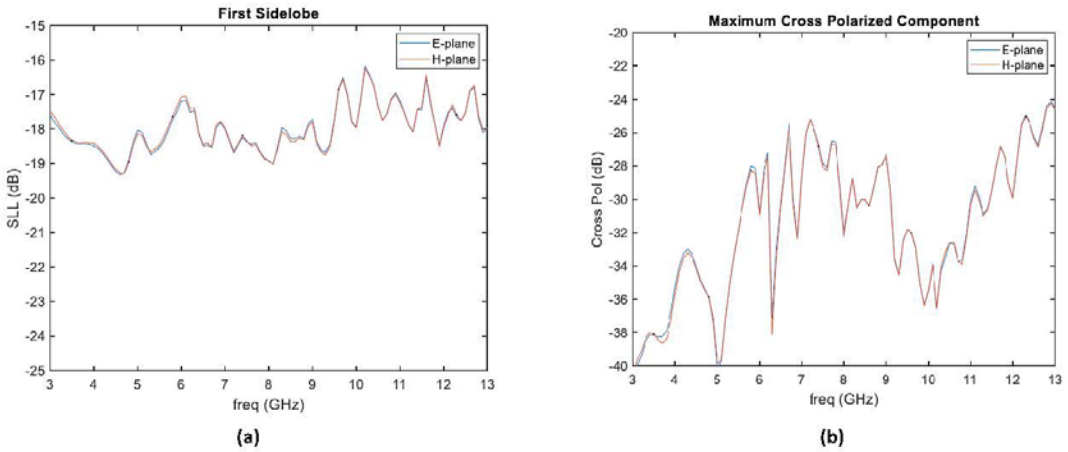

Figure 8. (a) First sidelobe level below peak of antenna pattern, (b) Crosspolarization level.

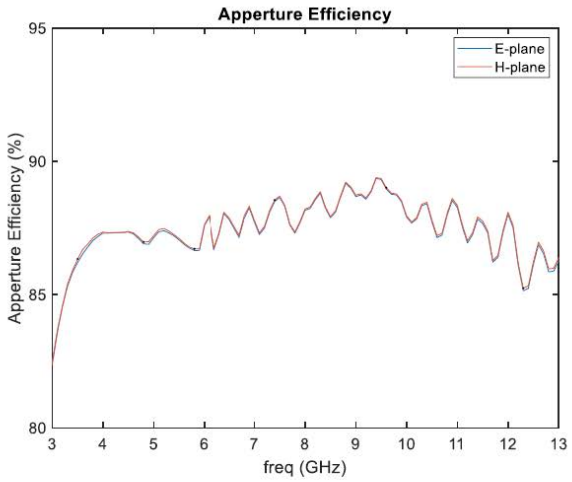

Figure 9. Aperture efficiency with the CSIRO QRFH.

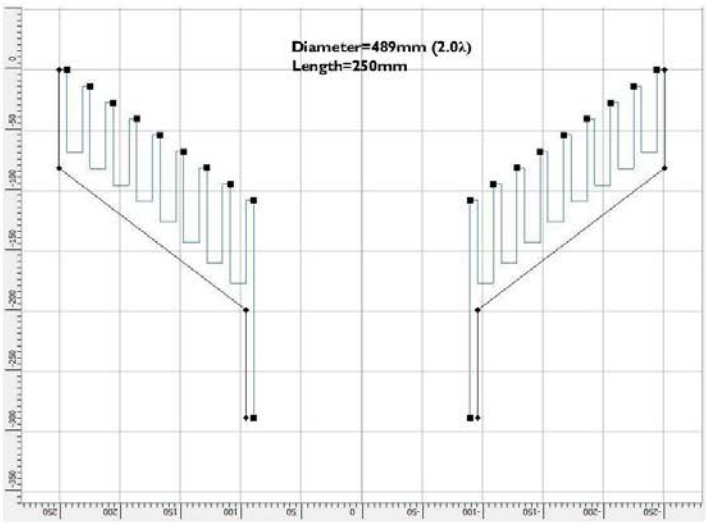

Figure 10. Axially corrugated feed horn (ACFH), 1.2 to 3.5 GHz.

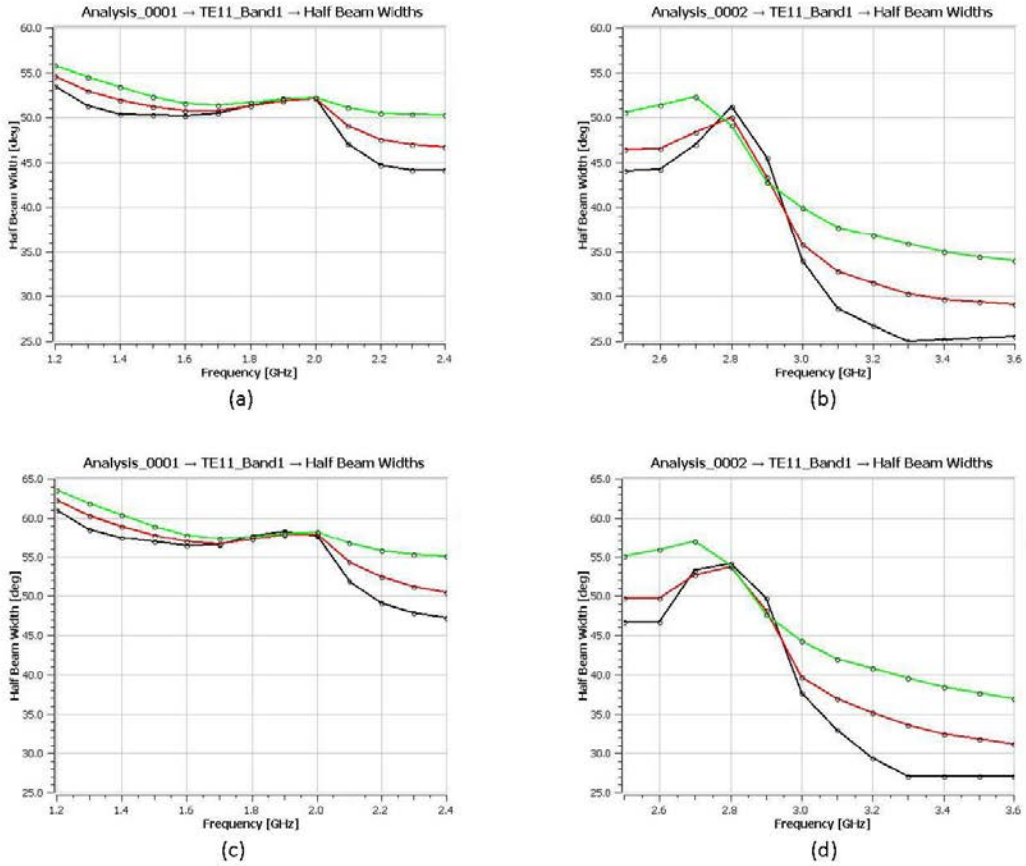

Figure 11. (a), (b) Half-beamwidth at -15 dB, (c), (d) Half-beamwidth at -18 dB. Green: H-plane, Red: 45º-plane, Black: E-plane.

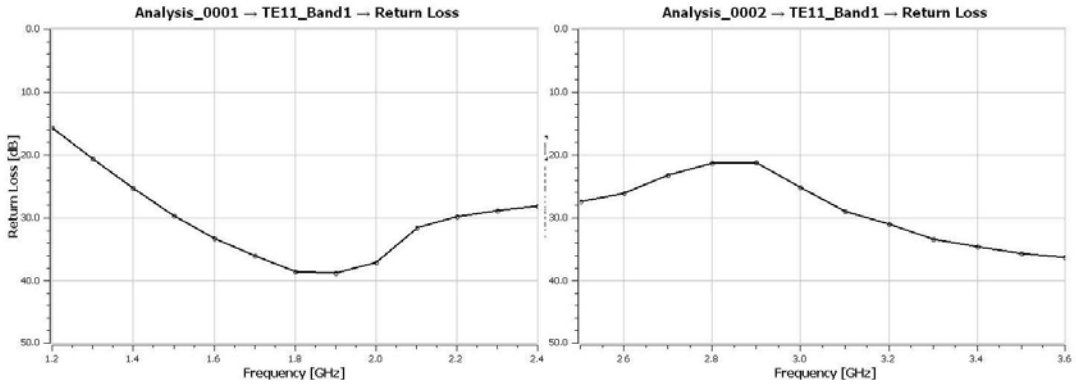

(a)

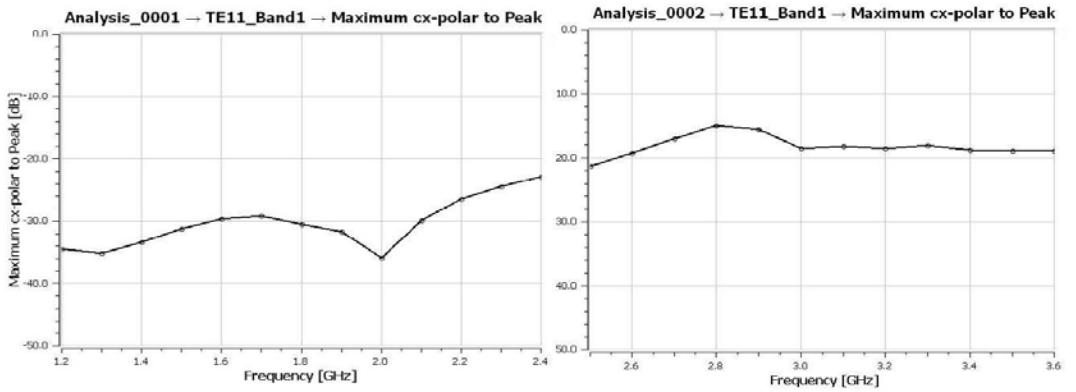

(b)

Figure 12. (a) Return loss, (b) Maximum crosspolarization.

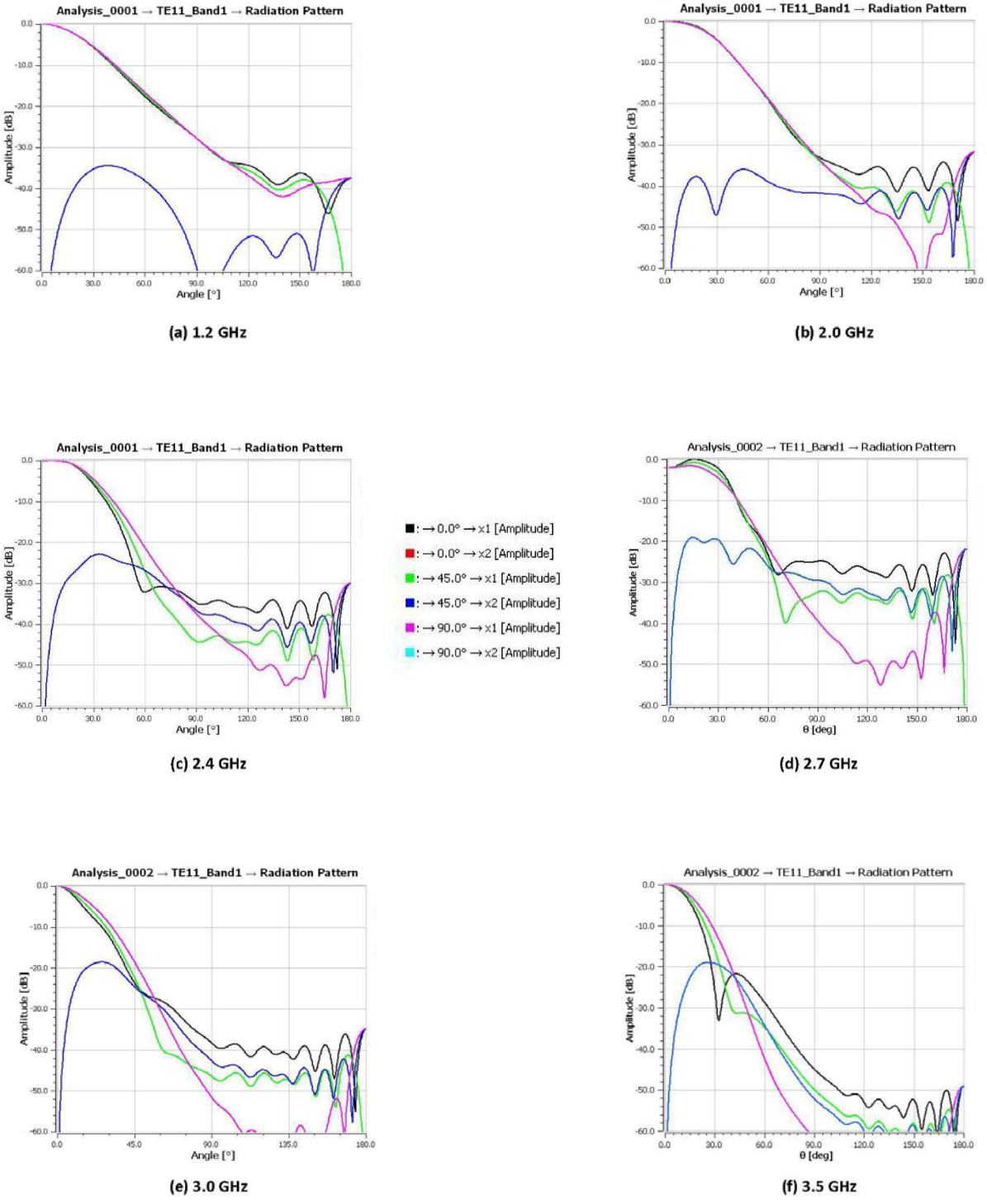

Figure 13. Simulated patterns of the 1.2 to 3.5 GHz ACFH.

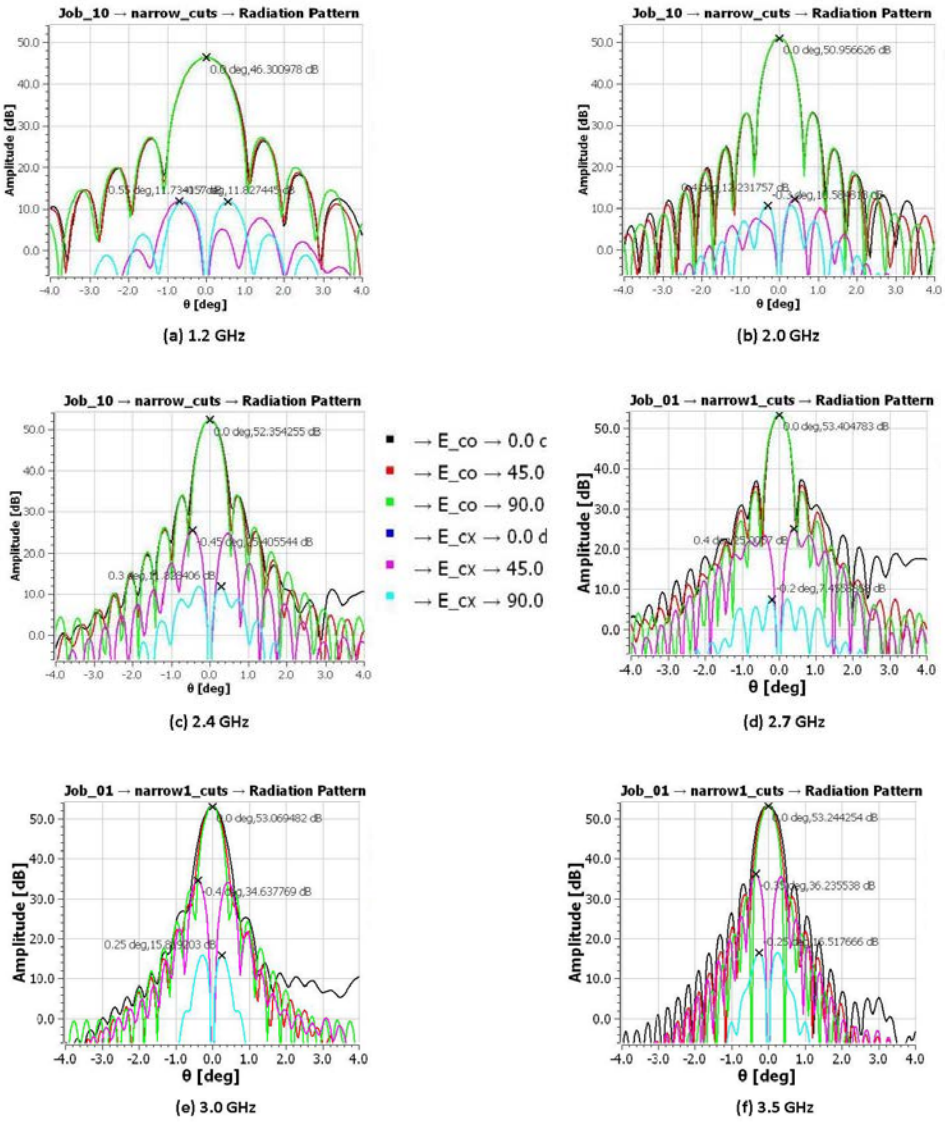

Figure 14. Simulated antenna patterns with the 1.2 to 3.5GHz ACFH.

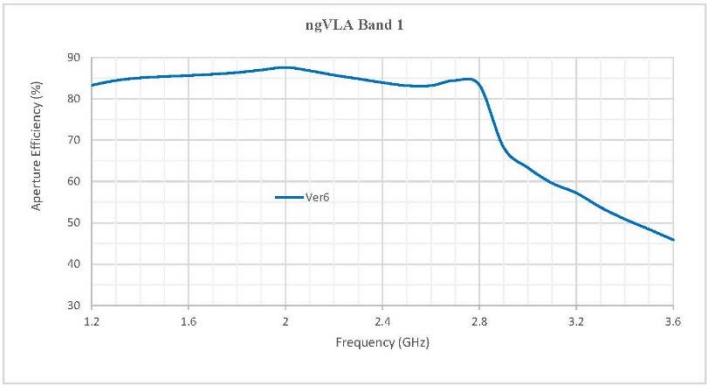

Figure 15. Aperture efficiency with the 1.2 to 3.5 GHz ACFH.

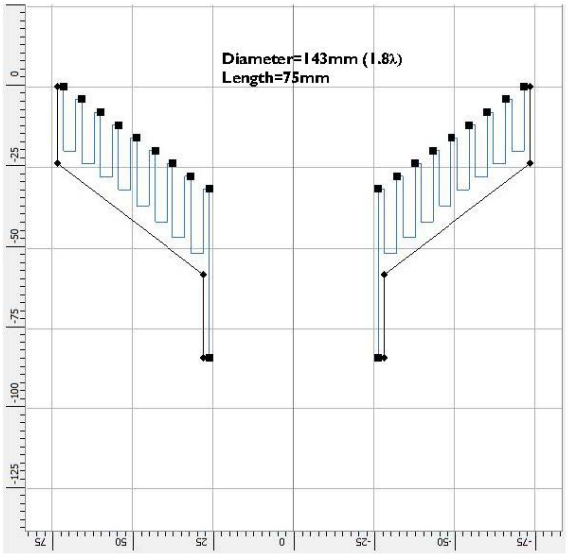

Figure 16. Axially corrugated feed horn, 3.5 to 12.3 GHz.

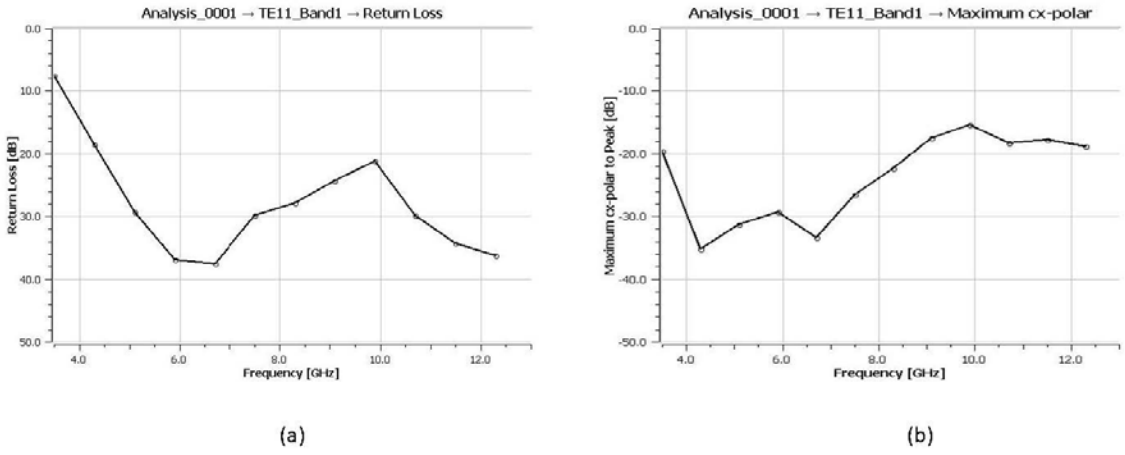

(a) (b)

Figure 17. (a) Return loss, (b) Maximum crosspolarization.

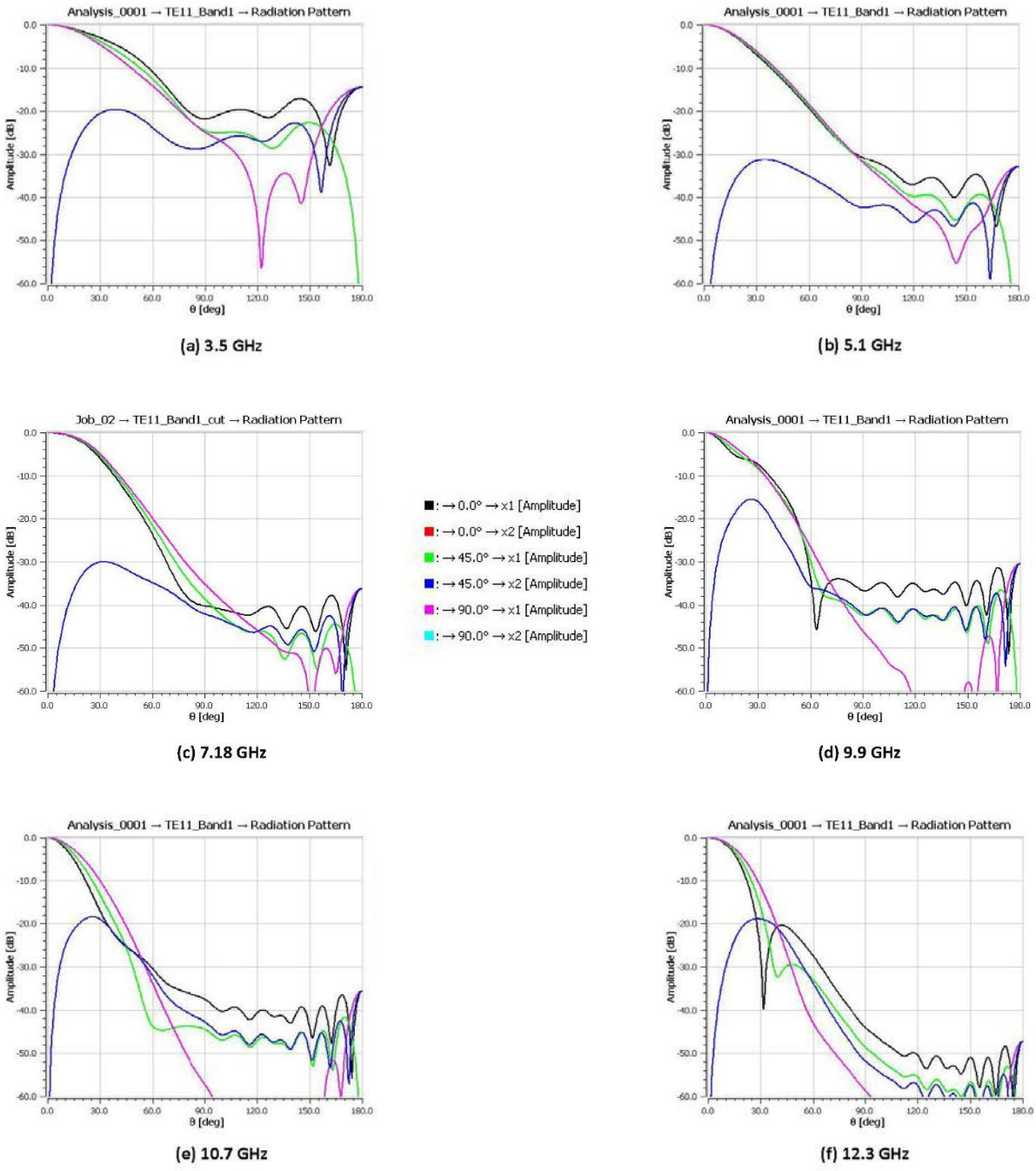

Figure 18. Simulated patterns of the 3.5 to 12.3 GHz ACFH.

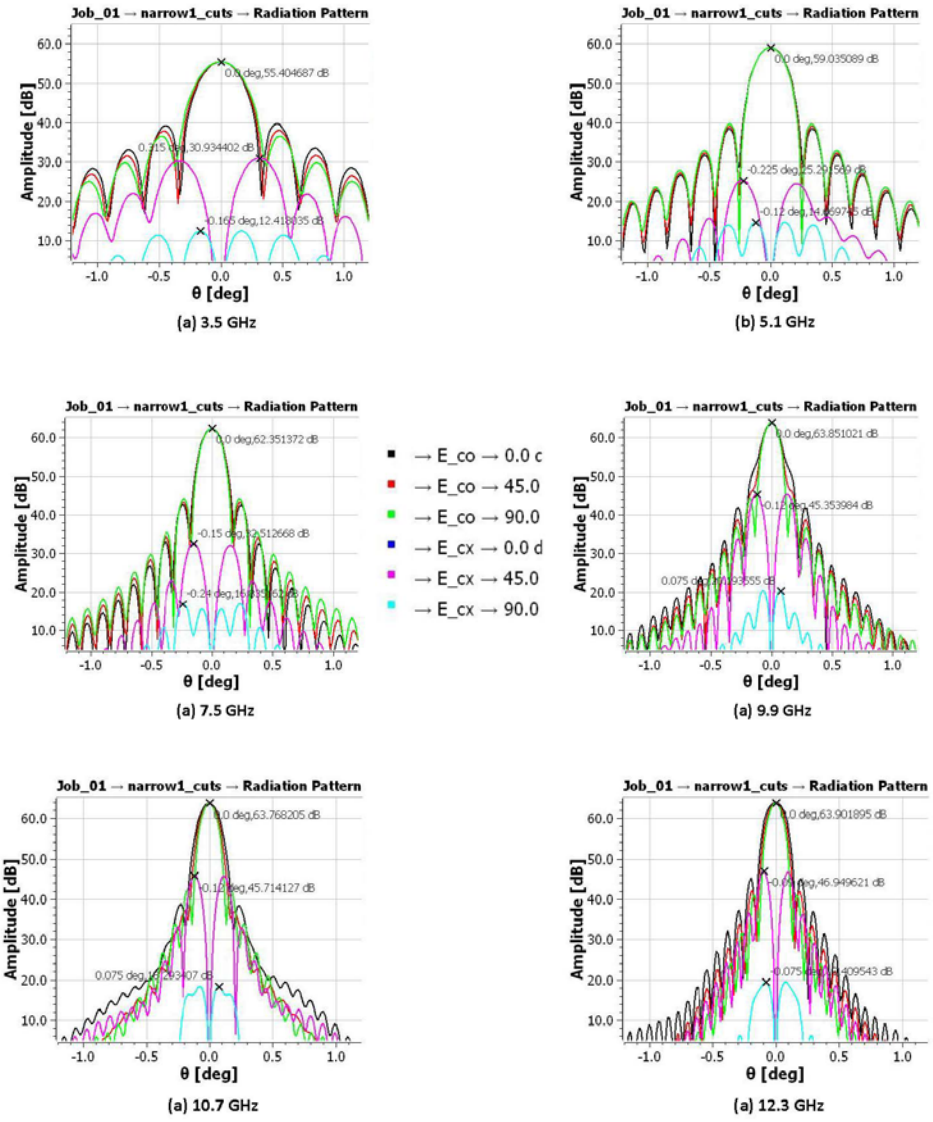

Figure 19. Simulated antenna patterns with the 3.5 to 12.3 GHz ACFH.

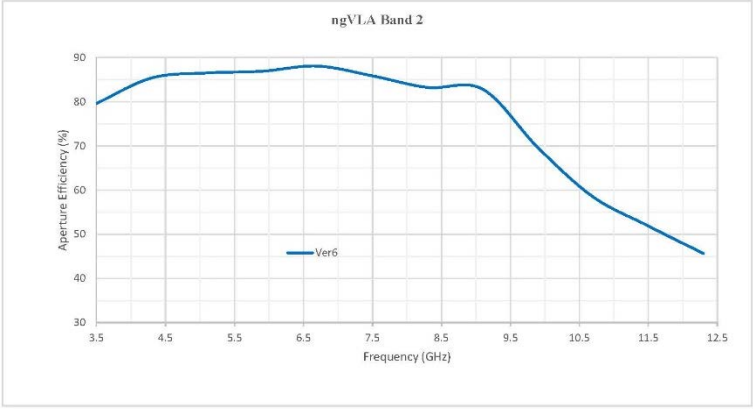

Figure 20. Aperture efficiency with the 3.5 to 12.3 GHz ACFH.

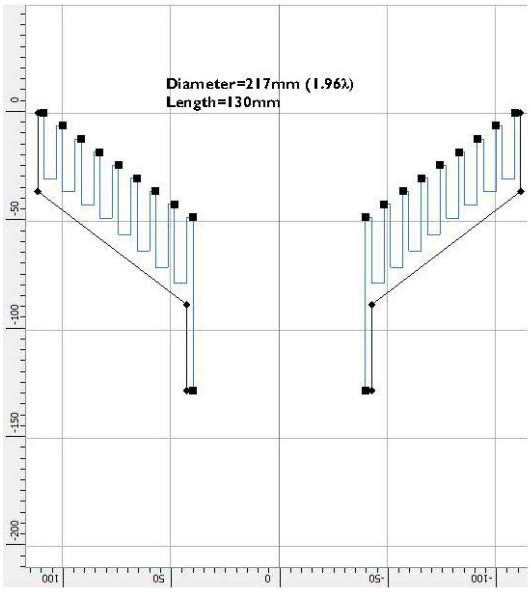

Figure 21. Axially corrugated feed horn, 2.7 to 5.8 GHz.

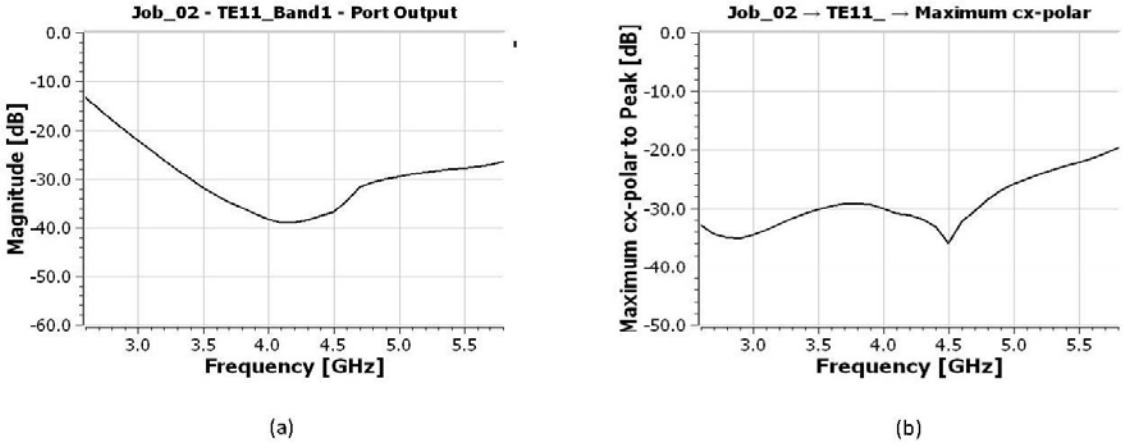

Figure 22. (a) Return loss, (b) Maximum crosspolarization.

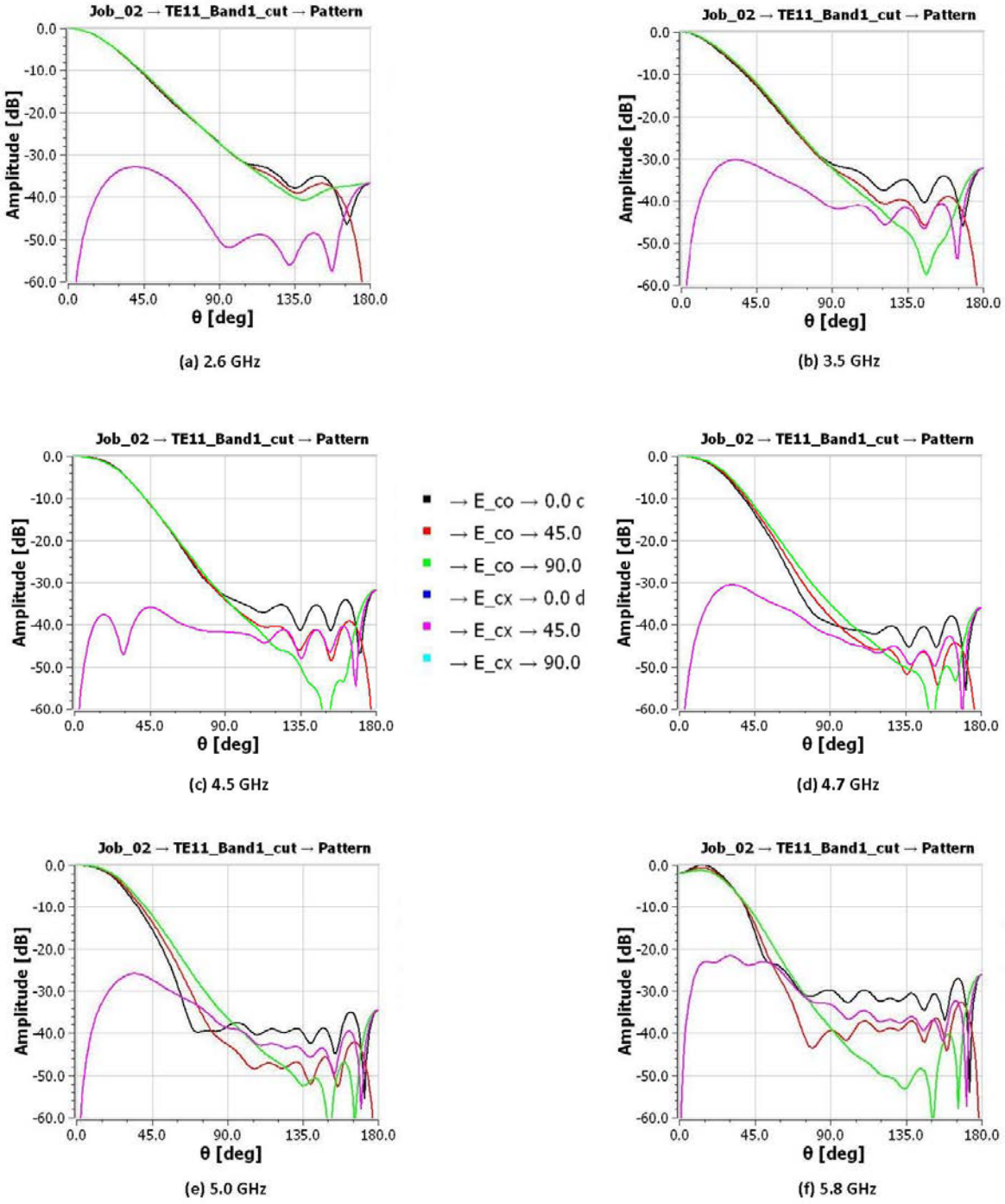

Figure 23. Simulated patterns of the 2.7 to 5.8 GHz ACFH.

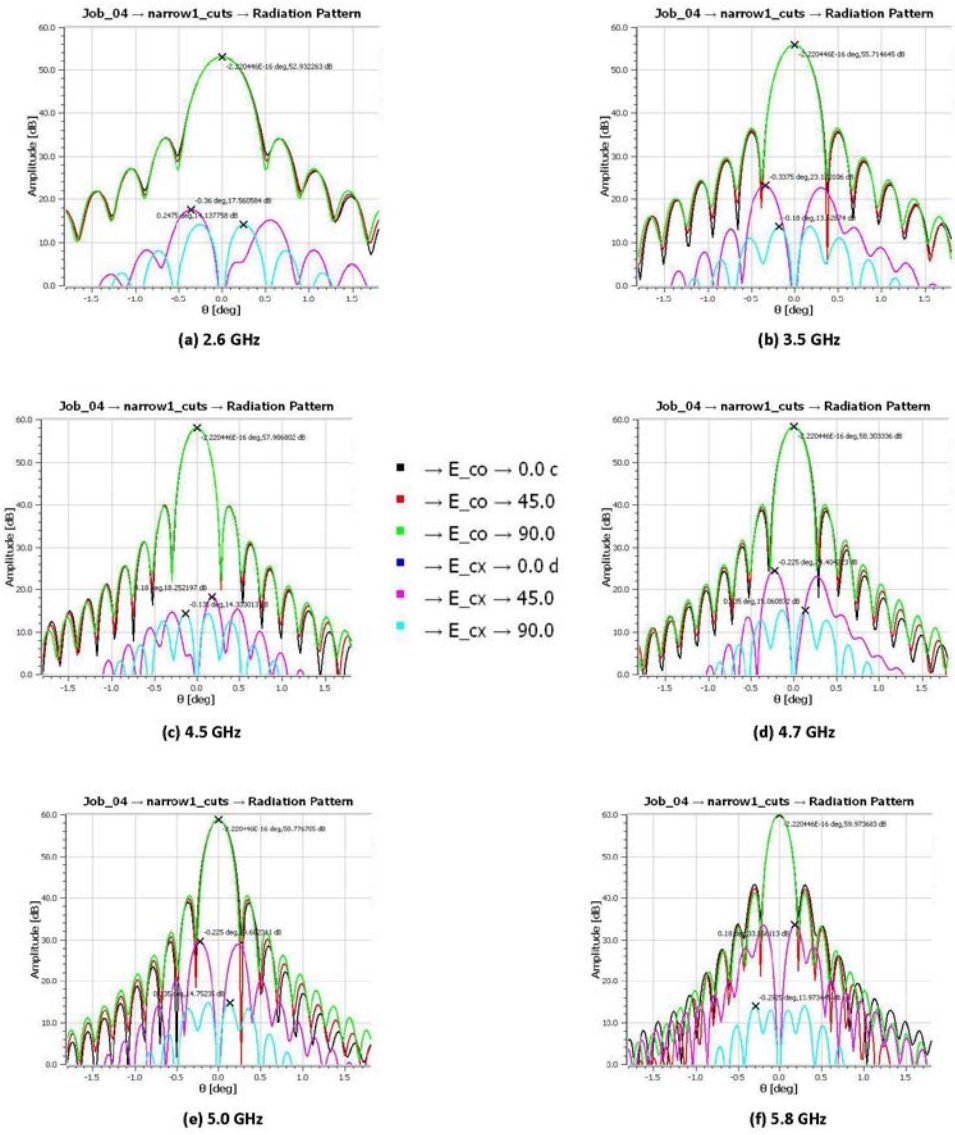

Figure 24. Simulated antenna patterns with the 2.7 to 5.8 GHz ACFH.

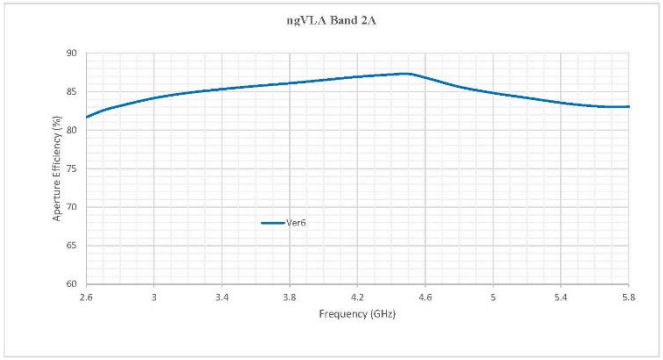

Figure 25. Aperture efficiency with the 2.7 to 5.8 GHz ACFH.

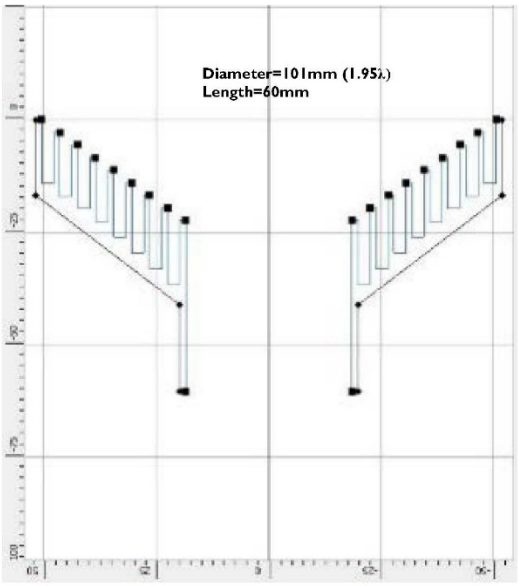

Figure 26. Axially corrugated feed horn, 5.8 to 12.3 GHz.

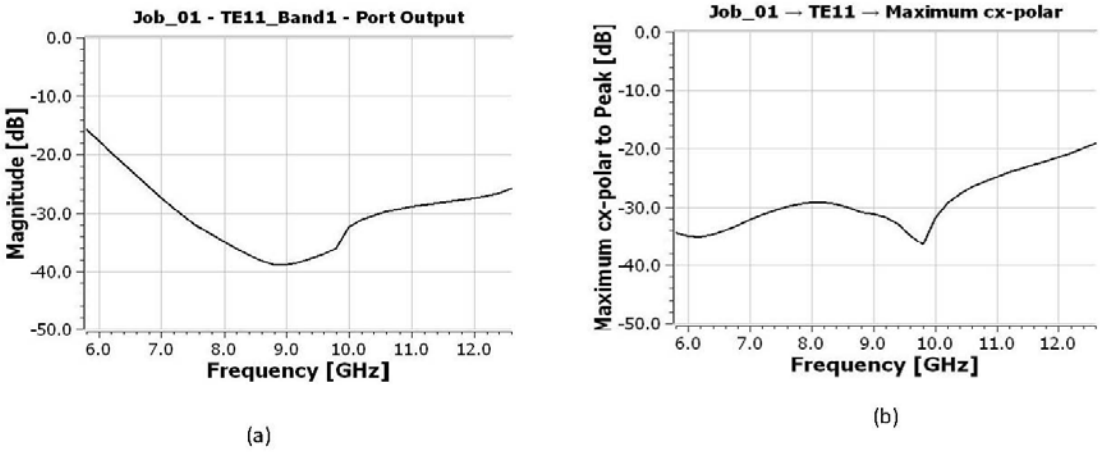

Figure 27. (a) Return loss, (b) Maximum crosspolarization.

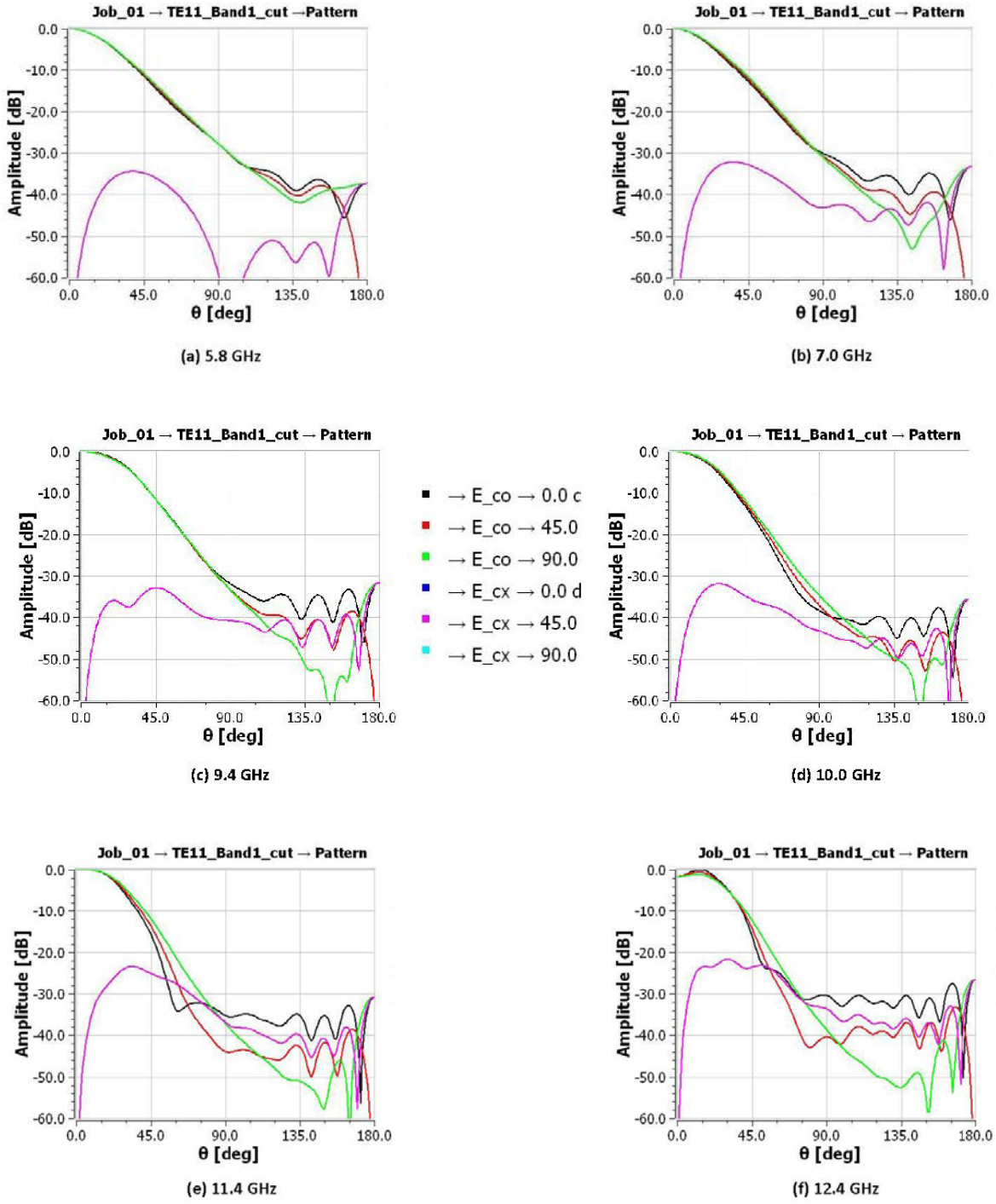

Figure 28. Simulated patterns of the 5.8 to 12.3 GHz ACFH.

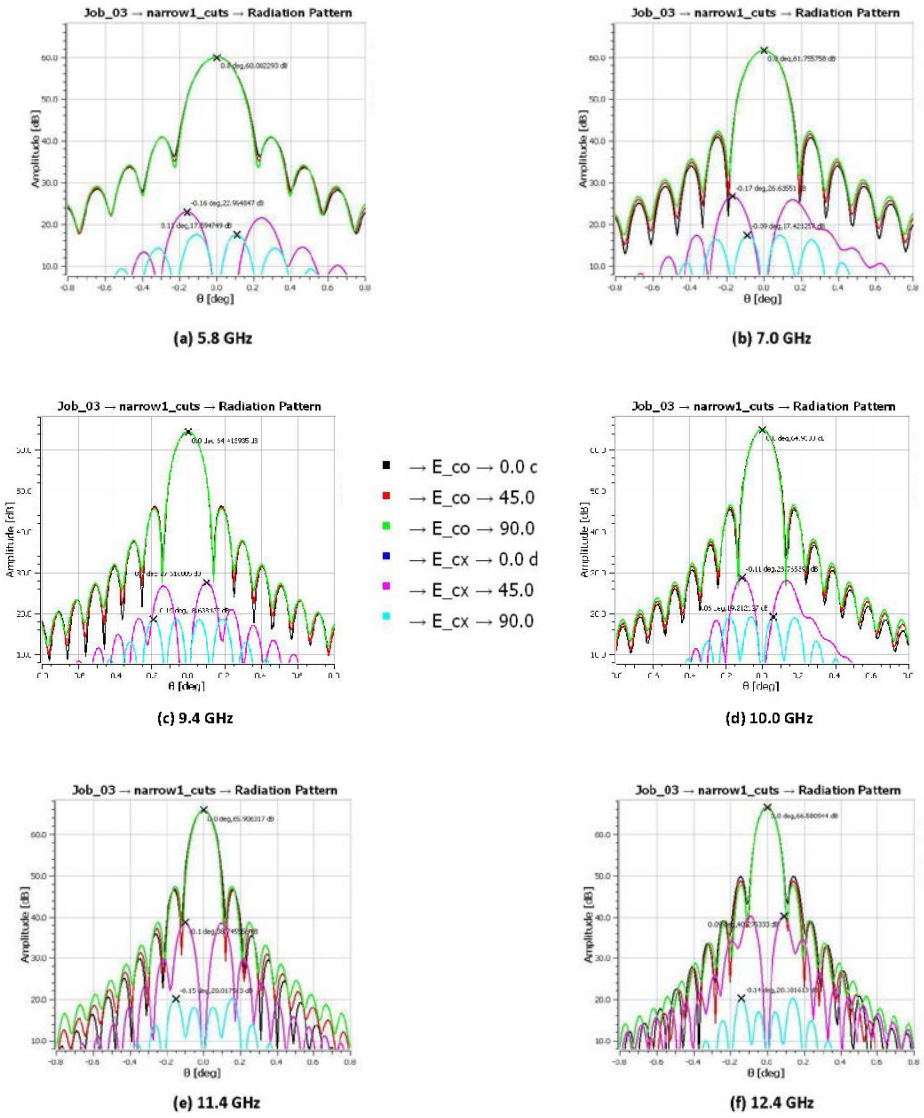

Figure 29. Simulated antenna patterns with the 5.8 to 12.3 GHz ACFH.

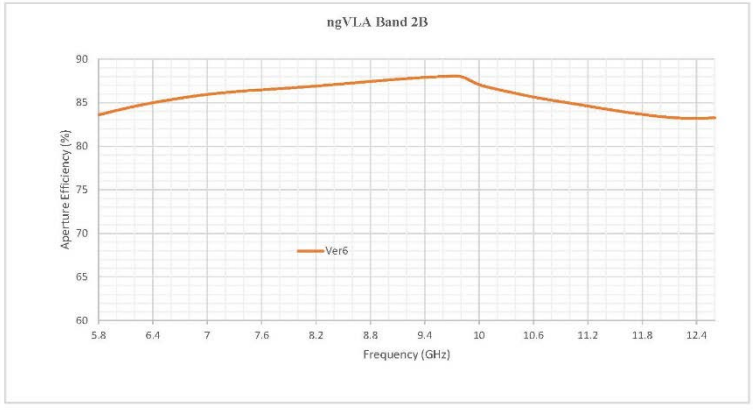

Figure 30. Aperture efficiency with the 5.8 to 12.3 GHz ACFH.

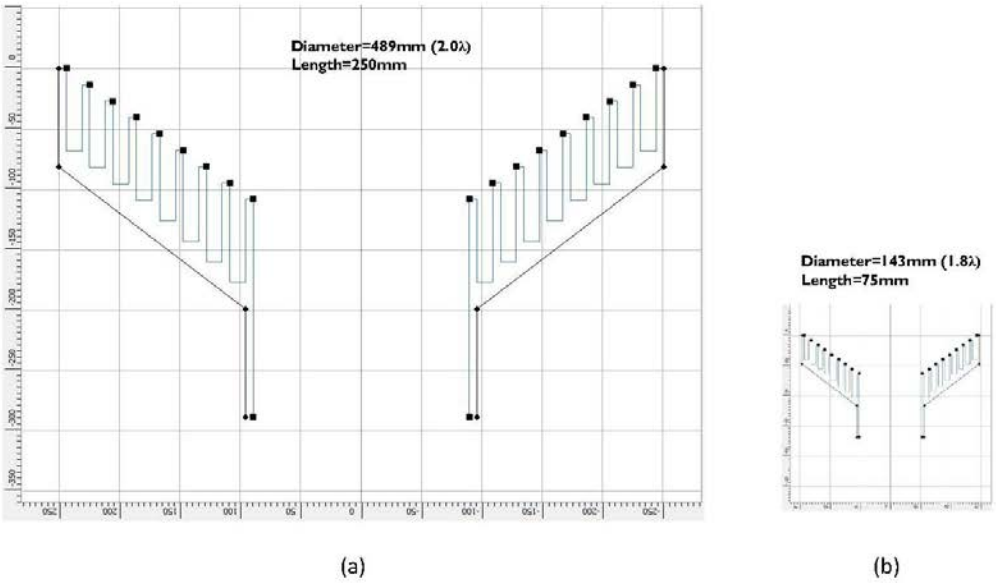

Figure 31. ACFHs for (a) 1.2 to 3.5 GHz, (b) 3.5 GHz to 12.3 GHz.

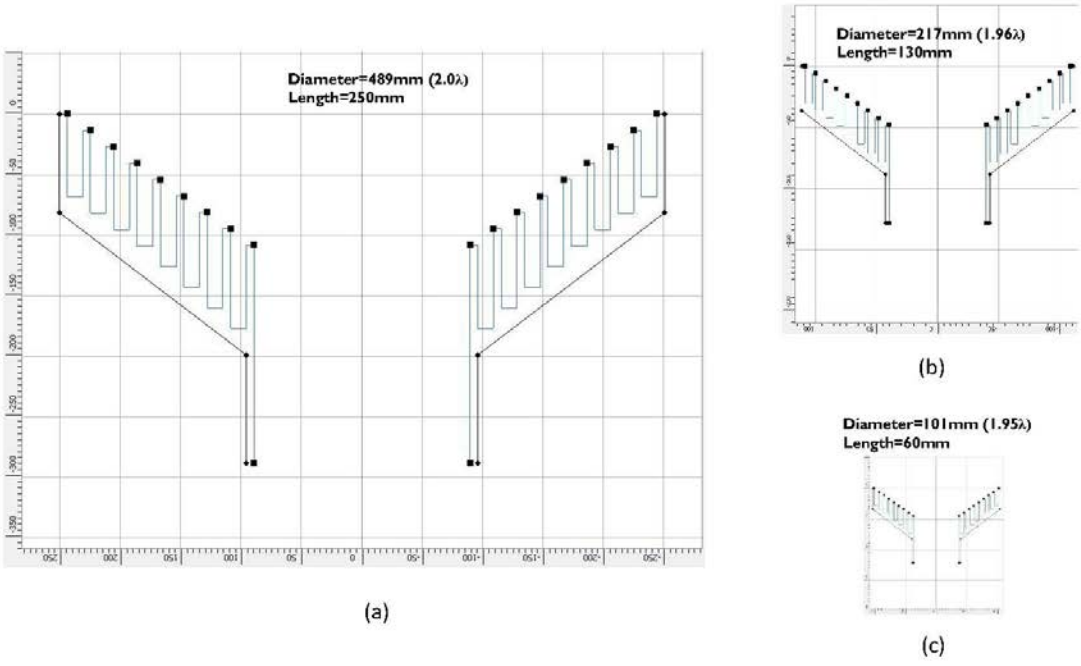

Figure 32. ACFHs for (a) 1.2 to 2.7 GHz, (b) 2.7 to 5.8 GHz, (c) 5.8 to 12.3 GHz.